ELSEVIER

Polymer 40 (1999) 1313–1323

polymer

An ab initio study of the structural and physical properties of a novel rigid-rod polymer: PIPD

J.C.L. Hageman*, J.W. van der Horst[1], R.A. de Groot

ESM Group, Research Institute of Materials, University of Nijmegen, Toernooiveld 1, 6525ED Nijmegen, The Netherlands

Received 6 March 1998; revised 30 March 1998; accepted 29 April 1998

Abstract

In this article, we present the first ab initio calculations on the novel rigid-rod polymer PIPD using density functional techniques. The behaviour of the molecular chain under strain is studied and the chain modulus agrees excellently with experiment. Two crystal structures are considered and hydrogen bonding networks as proposed from X-ray diffraction measurements are demonstrated to exist. Negligible energy differences were found and both structures could exist at room temperature.

The electronic structure reveals a $\pi - \pi$ interaction like in graphite, resulting in a weak bonding. The interaction due to the hydrogen bonding network is smaller, however: it leads to a significantly larger bonding energy. As the interchain bonding in PIPD is approximately 3 times the bonding without the network, the improvement in the compressive strength of PIPD compared to PBO and PBT can be attributed to the hydrogen bonding network.

Keywords: Rigid-rod polymer fibre; PIPD; Electronic structure

1. Introduction

Rigid-rod polymers, like poly-(*p*-phenylene benzobisoxazole) (PBO) and poly-(*p*-phenylene benzobisthiazole) (PBT), are high-performance polymers which have excellent tensile properties. The fibres processed from these polymers have moduli of the order of 300 GPa, due to the high stiffness of the polymer chains (hence the intrachain interactions) and the high molecular orientation. The properties of these fibres under compression are, however, not impressive.

The latter properties mainly depend on the interchain bonding, which, in PBO and PBT, is only due to the weak Van der Waals interactions. Poly-(*p*-phenylene terephthalamide) (PpTA) possesses a somewhat higher compressive strength due to a unidirectional hydrogen bonding network. The introduction of intermolecular hydrogen bonding into a rigid-rod polymer is expected to lead to an improved compression behaviour.

Recently a novel rigid-rod polymer was created by Akzo Nobel Central Research, namely poly-{2,6-diimidazo[4,5-b:4'5'-e]pyridinylene-1,4(2,5-dihydroxy)phenylene}, referred to as PIPD (or M5) [1–3]. Based on X-ray fibre diffraction data, a monoclinic crystal structure was proposed with a bidirectional hydrogen bonding network [2]. Experiments indicate that PIPD has tensile properties comparable to those of PBO and PBT, and that the much higher compressive strength is due to this hydrogen bonding network.

It is difficult to establish the positions of the hydrogen atoms with X-ray diffraction (XRD), especially if the material has a low crystalline perfection. Moreover, XRD cannot provide information on the mechanical, optical and electronic properties of the polymer and the influence of the hydrogen bonding network on these properties.

To provide this additional information on PIPD, calculations were performed at an ab initio level. There are several reasons to choose the ab initio level. Firstly, it has been shown that ab initio calculations provide good results for mechanical properties of polyethylene [4] and PBO [5].

A more important argument for using ab initio calculations is the complexity of crystals of conjugated polymers in general and PIPD in particular. Welsh et al. [6] have discussed the balance between the conjugation in PBO and PBT and the steric hindrance which may lead to a non-zero torsion angle. Ambrosch-Draxl et al. [7] have shown in poly-(para-phenylene) (PPP) that interchain

* Corresponding author. Tel. +31-243652805; Fax: +31-243652120

[1] Present address: Theory of Materials and Industrial Processes, Technical University Eindhoven, PO Box 513, 5600MB Eindhoven, The Netherlands.

0032-3861/98/$ - see front matter
PII S0032-3861(98)00344-9

interactions can decrease this torsion angle (from 27° for an isolated chain to 17° in the crystal structure). They have also shown that the bandgap is sensitive to this torsion angle, while properties like the chain modulus might also depend on it.

Since in PIPD the torsion angle will be set by a subtle balance between steric hindrance, interchain interactions (including hydrogen bonds) and the conjugation, an ab initio method is required to evaluate the structure of PIPD and its properties. Since we are interested in the properties of crystalline PIPD, the Car–Parrinello technique, based on Density Functional Theory, with periodic boundary conditions is used.

In Section 2, we discuss the computational method used. The subsequent section discusses the molecular chain of PIPD and its behaviour under strain. Section 4 is dedicated to the monoclinic crystal structure as determined from XRD [2] and its electronic and optical properties. In Section 5 the triclinic structure also proposed based on XRD data [2] is compared with the monoclinic structure. Section 6 gives a short overview and discussion of the influence of gradient corrections for PIPD, and the final section presents the conclusions.

2. Computational method

Density Functional Theory is used to describe the electron–electron interactions. The ground state properties would be described exactly in DFT if the exchange-correlation energy (E_{xc}) were known exactly. Unfortunately, E_{xc} has to be approximated, but good approximations are known. The local density approximation (LDA) [8] is widely used and gives excellent results for first-order bonds in most cases. Also gradient corrections (GC) to LDA have been developed (GGAII [9] and Becke–Perdew (BP) [10], amongst others). The second-order bonds, like the hydrogen bond which is important in the case of PIPD, are described better by these [11]. However, bulk properties seem to be less accurate [12]. As there is little experience with gradient corrections in polymer systems, both LDA and GCs are applied (self-consistently). For the geometry optimisation, both BP and GGAII are used as GCs; for the band structure calculation only GGAII is used.

To perform geometry optimisations, an ab initio Molecular Dynamics scheme is used as it is implemented in the fhi96md code [13]. A damping scheme is used which means that kinetic energy is extracted until the ground state geometry for $T = 0$ K is reached. The forces necessary for the dynamics are calculated from the electronic structure using the Hellmann–Feynman theorem. The electronic wave functions are found by solving the Kohn–Sham equations [14] with an iterative scheme [15]. Troullier–Martins norm-conserving pseudopotentials [16] are used in the fully separable form [17] to describe the atomic cores. The radii used for carbon, nitrogen, oxygen and hydrogen are 1.3, 1.4, 1.4 and 0.4 in atomic units. Whenever a gradient correction is applied, the pseudopotential is also created with this XC-functional to describe correctly the exchange-correlation between core-electrons and valence-electrons. The wave functions are expanded in a plane wave basis set. Only waves for which $|\mathrm{k} + \mathrm{K}|^2 \leq E_{cut}$ are included. An E_{cut} of 55 Ry was necessary which leads to 26 000 plane waves for the monoclinic crystal. Brillouin zone averages were calculated as a summation of two special k-points, unless stated otherwise.

3. The monomer and molecular chain

The repeat unit of PIPD is drawn schematically in Fig. 1. Compared to trans-PBO, the most important differences are the OH groups added to the phenyl group and the replacement of the oxygens in the benzobisoxazole group of PBO by NH groups. Due to these replacements, there are four hydrogen atoms which may form hydrogen bonds.

The repeat unit consists of two ring systems: the dihydroxyphenylene group, here referred to as the Ph group, and the diimidazopyridinylene group, referred to as the DIP group or DIP ring system. These groups are connected by a CC bond. As already mentioned, a rotation around this bond might be possible, like in PBT.

Before turning to the crystalline form of PIPD, the isolated molecular chain is studied. For this purpose, an

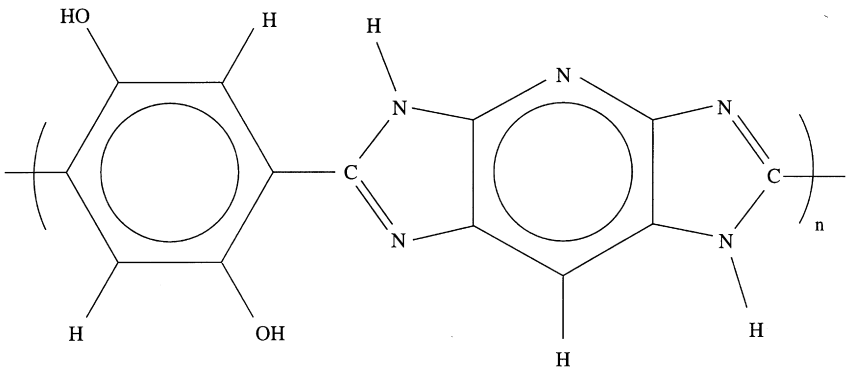

Fig. 1. The structural formula of PIPD.

Table 1
Some important bond lengths and the torsion angle for the single chain

Bonds	LDA	GGAII	BP	Comment
C–C	1.381–1.422	1.394–1.432	1.403–1.450	In dihydroxyphenylene group
C–C	1.377–1.427	1.390–1.434	1.400–1.456	In heterocyclic group
C–N	1.318–1.334	1.333–1.350	1.346–1.364	Double bond
C–N	1.362–1.377	1.384–1.393	1.391–1.403	Heterocyclic bond
C–C	1.427	1.452	1.452	Connecting the rings
O–H	1.032	1.009	1.021	N side
O–H	1.040	1.016	1.027	CH side
H···N	1.617	1.725	1.698	N side
H···N	1.548	1.635	1.621	CH side
N–H	1.022	1.016	1.031	N side
N–H	1.021	1.015	1.030	CH side

orthorhombic super cell was used with periodic boundary conditions: the axes perpendicular to the chain axis (c) were chosen to be so large ($a = 9.5$ Å and $b = 4.7$ Å) that there was no chain–chain interaction. The length in the chain direction was optimised ($c = 12.03$ Å, 12.16 Å and 12.18 Å for LDA, GGAII and BP respectively). In this super cell, the geometry of the molecular chain was optimised for all three functionals: LDA, BP and GGAII. Some important bond lengths are listed in Table 1. In this table, two sides of the chain are discriminated. One side has an N atom in the DIP ring system, the other a CH group (Fig. 1).

The CC bonds in the Ph ring have lengths ranging from 1.38 to 1.42 Å (in LDA). In the DIP ring system, the CC bonds perpendicular to the chain direction have lengths of 1.42 and 1.43 Å and the others of 1.38 and 1.39 Å. The CN distances can be divided into two groups: the bonds which are indicated in Fig. 1 as double or aromatic have a length of approximately 1.33 A, the others of 1.37 Å. This can be compared with standard values [18] for single, aromatic and double CC bonds, which are respectively 1.54, 1.40 and 1.34 Å, and for heterocyclic and double CN bonds, which are respectively 1.35 and 1.32 Å. These distances are consistent with the schematic picture in Fig. 1.

The symmetry of the pyridine group in the DIP ring system is slightly distorted due to the trans arrangement of the imidazo groups: the CN bond on the left-hand side of the pyridine group (Fig. 1) is 0.016 Å shorter than the CN bond on the right-hand side. Considering the CC bonds perpendicular to the chain, the one on the left-hand side is the shorter (by 0.006 Å). The CC bond at the bottom on the right-hand side is 0.008 Å shorter than the CC bond on the left-hand side.

The connection between the two ring systems is a CC bond with a length of 1.43 Å (in LDA). Hence, one may conclude that this is not a single bond but that it has a sizable degree of aromatic character. In PPP, a similar connecting bond is found with a distance of 1.456 Å [7].

In LDA, the hydrogen atoms which are bonded to the oxygen atoms are only at a distance of approximately 1.6 Å from the nitrogen atoms in the DIP ring system. Also, the OH distance is 1.04 Å, which is 7% larger than the OH distance in phenol calculated in LDA (0.975 Å [19]). Similar results can be seen in the GGAII and BP calculations, although somewhat less pronounced. From this, it is clear that the hydrogen atoms bonded to the oxygen atoms form an internal hydrogen bond with nitrogen.

There is a difference between the two H···N distances (0.07 Å) which can be understood from the fact that the CNC group in the DIP ring system differs from the opposite lying CCC group. Therefore the nitrogen atoms will be pulled more inwards on the side of the CNC group than on the other side. For this reason, the H···N distance is longer on the CNC side of the chain.

The two ring systems both lie in the *ac* plane, which means that the torsion angle is zero. A check was performed as to whether the flat structure is really the ground state and not a metastable state, by calculating the energy of a structure with a torsion angle of 10°. This structure had a 57 meV higher energy and the angle reduced under relaxation. Hence, the flat structure is the ground state. This can be understood by realizing that the conjugation and the internal hydrogen bond will both tend to a flat chain. The only opposing force might result from the steric hindrance between the two hydrogen atoms on the different groups, which is expected to be small.

3.1. Mechanical properties

One of the important mechanical properties of the fibres is the elastic modulus of a polymer chain, i.e. the chain modulus. As this modulus mainly depends on the intramolecular interactions, it can be calculated at a single chain level. The validity of this single chain approximation is discussed below.

The chain modulus (Y_c) is defined as

$$Y_c = \frac{L_0}{A}\frac{d^2E(L)}{dL^2}\bigg|_{L=L_0} \quad (1)$$

Here, $E(L)$ is the total energy curve, which can be calculated by a geometry optimisation for super cells as described above with different lengths L. L_0 is the equilibrium unit

cell length which can be calculated from the total energy curve. A is the area per chain which is calculated from the volume of the experimental unit cell [2] divided by the experimental length of the monomer ($A = 20.78$ Å^2).

Ten unit cell lengths were used to calculate the energy curve and this resulted in theoretical values for the chain modulus of 578, 553 and 558 GPa for the LDA, GGAII and BP functionals, respectively. These calculated values are in agreement with the experimental value of the chain modulus [3] (510 ± 60 GPa), considering the fact that the chain in the calculations is infinitely long, which is an ideal case. For this reason, the ab initio value is an upper bound.

Clearly, we have neglected interchain interactions and the validity of this procedure should be discussed. The interchain interaction might influence the backbone of the chain and cause a rotation around the connecting CC bond. This can affect the modulus by two effects. First, the rotation will reduce the strength of the CC bond, but only the π contribution to it, as the σ part is not affected by a rotation around the bond. The reduction in the overlap of the p-orbitals which form the π bond can be estimated to behave like a cosine of the rotation angle. This means that the reduction in the strength of the CC bond due to a rotation of approximately 10° will be less than 1% and this effect may be considered small.

Second, the rotation of the groups will weaken the internal hydrogen bond, as the H···N distance will increase. The maximum size of this effect was estimated by calculating the chain modulus of a hypothetical polymer in which the OH group of PIPD is substituted by a hydrogen atom. In this case, no internal hydrogen bond can be formed. Using the same area per chain A in Eq. (1), the difference in chain modulus between the hypothetical polymer and PIPD is a measure of the maximum effect of the internal hydrogen bonds. For LDA, this difference is 40 GPa, an effect of 7%. Of course, the actual weakening of the hydrogen bond will be much lower.

Hence, the upper bound to the effect of the interchain interaction on the modulus can be estimated to be an 8% reduction of the modulus. This gives a validation of the single chain approach.

The actual modulus of the fibre will be lower than the calculated chain modulus. This is due to the fact that in the calculations infinite chains are used and that in the actual fibre the chains are not perfectly aligned to the direction of the fibre axis. The latter effect, however, is already taken into account in the experimental value by an extrapolation procedure [3] and hence should not be included in the discussion of the discrepancy between the theoretical and experimental value of the modulus.

3.2. Deformations due to strain

It is interesting to study the influence of strain on the bond lengths and angles. To evaluate this, the strain of some groups in the monomer is plotted versus the strain applied to the molecular chain (Fig. 2).

First, we consider the groups which form the backbone: the Ph group, the CC bond which connects the two ring systems, and the DIP ring system. As they are all in the backbone, they all participate in the elongation of the chain but not necessarily to the same extent. To visualise this, the strain–strain curve of the monomer is also plotted (dotted line). Under positive strain, one can see that the Ph group is the least stiff, followed by the CC bond. The DIP ring system is the stiffest one. As the DIP ring system is a large group, we also plotted the behaviour of the pyridine group which is similar to the behaviour of the total DIP group. This implies that the imidazo groups also behave the same. The behaviour under negative strain is not really different, only in this case the CC bond is somewhat stiffer than the total chain.

It is somewhat unexpected that the Ph group is the weakest link and not the CC bond. The CC bond is almost aromatic like the CC bonds in the Ph group. As there is only one connecting bond between the rings and there are two CC bonds in the Ph group in the chain direction, one would think that it would be easier to deform the connecting bond. And indeed, this is true. However there are also angles which contribute to the strain. In particular, the CCC angle where the middle carbon atom is the one which is also in the connecting CC bond. When a strain of 2.6% is applied, this angle decreases from 120° at equilibrium to 116°. For a CC bond length of 1.394 Å, the contribution to the length of the chain increases from 0.697 to 0.736 Å, which is an increase of 5.6% solely due to the decrease of the angle (it is 6.3% if one takes the change in the bond length into account). The increase of the CC bond in the Ph group is only 1.2% for a strain of 2.6% of the monomer. Together this leads to a strain of 3.7% of the Ph group. The strain on the CC connection bond is 3.0%.

In the DIP group, the angles all change less than 1.5%, except the CNC and CCC angle in the pyridine group, which both change 2%. The first phenomenon can be explained from the fact that the angles in the imidazo groups are already under tension. The CCC angle in DIP behaves the same as the CCC angles in the Ph group which are not centred around the chain axis. Together with the generally shorter bonds in the DIP system, this results in a low contribution to the elongation.

Next, the two interesting bonds which are not in the backbone are to be considered. The OH bond and the H···N bond form the internal hydrogen bond. These bonds behave differently to the applied strain.

For positive strain on the chain, the OH bond becomes shorter and a negative strain results in an elongation. The H···N bond is elongated for positive strain in a highly nonlinear way and is clearly weaker than the monomer as a whole. A negative strain gives a shorter distance and the bond is easier to deform than the monomer.

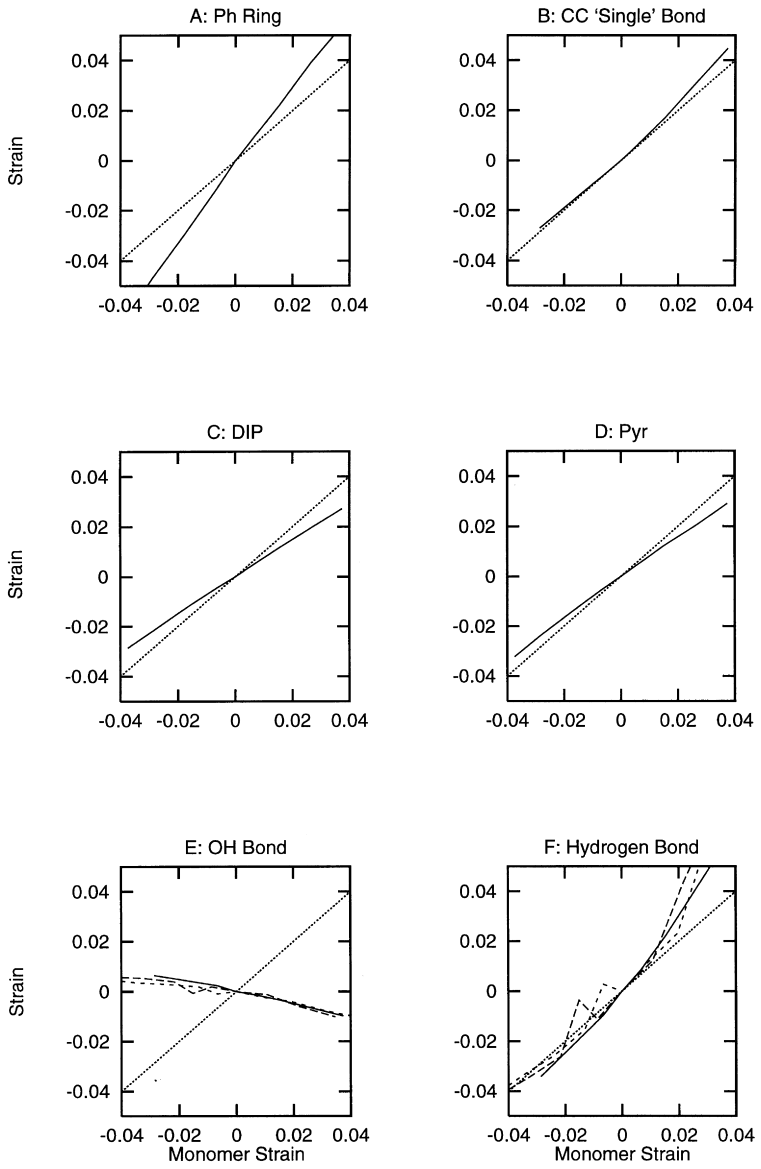

Fig. 2. The strain of specific groups as a function of the strain of the monomer. The nomenclature of the groups is given in the text. The solid lines are LDA results. The large dashed lines are the results with the Becke–Perdew functional and the small dashed lines those with the Perdew–Wang functional. The dotted curve represents the strain of the monomer itself.

We can understand this behaviour from the fact that the hydrogen bond is only a second-order bond and hence an order of magnitude weaker than the other bonds. When the chain elongates, the DIP ring system will be at a larger distance from the Ph group and hence from the oxygen attached to this group by a first-order bond. The hydrogen will take a position somewhere between the oxygen and the nitrogen. As it is bonded to the oxygen with a first-order bond and with nitrogen with a second-order bond, it will always be closer to the oxygen. Hence an increase in distance between the oxygen and the DIP group will result in an increase in the H···N distance. This will weaken the bond and another increase in the H···N distance is the result. As the H···N is now weaker, it will not pull the hydrogen away from the oxygen as before and hence the OH bond will become shorter.

In the case of a negative strain, the process will be less pronounced as we have seen that the CC bond, which is the distance between the Ph group and the DIP group, will change less.

4. Monoclinic PIPD

Klop et al. [2] have performed X-ray diffraction studies to determine the crystal structure of PIPD. There are two crystal structures which give the observed diffraction pattern: a triclinic crystal structure containing one monomer per unit cell and a monoclinic with two monomers per unit cell. As the latter is the more plausible from temperature-dependent X-ray diffraction, we will first study the monoclinic crystal

Table 2
Some important bond lengths and the torsion angle for the monoclinic structure

Bond	Mono			Comment
	LDA	GGAII	BP	
C–C	1.380–1.417	1.382–1.422	1.390–1.437	In dihydroxyphenylene group
C–C	1.429	1.431	1.432	Connecting the rings
O–H	1.054	1.035	1.047	N side
O–H	1.092	1.066	1.083	CH side
H···N	1.583	1.610	1.595	N side, intrachain
H···N	1.467	1.495	1.483	CH side, intrachain
N–H	1.041	1.033	1.049	N side
N–H	1.047	1.028	1.044	CH side
H···O	1.955	1.935	1.894	CH side, interchain
H···O	1.860	1.856	1.807	N side, interchain
Torsion angle	10.2	10.2	10.2	

structure. The lattice parameters of the monoclinic unit cell are $a = 12.49$ Å, $b = 3.48$Å, $c = 12.01$Å, $\alpha = 90°$, $\beta = 107°$ and $\gamma = 90°$. The two monomers form two chains in the c direction crossing the *ab*-plane [20].

For the fixed unit cell, geometry optimisations of the chains were performed. The geometry used as a starting point was taken from the diffraction modelling from Klop et al. [2].

Some important optimised bond lengths are listed in Table 2 for all three XC functionals and also the torsion angle. The projections of the optimised geometry on the *ab*-plane and *ac*-plane are shown in Fig. 3. The influence of the interchain interaction on the backbone of the polymer is very small. Changes which occur in CC and CN bond lengths are all smaller than 0.7%. Changes in angles are negligible (smaller than 1°) except the change of the torsion angle. This angle this time is 10° and not zero as for the single chain, which is a significant change. The DIP group has rotated out of plane in contrast to the Ph group which still lies in the *ac*-plane in the monoclinic cell.

The NH distances grow (in LDA) 2 to 3% with respect to the single chain data, which is a clear influence of the interchain interaction. With gradient corrections, the growth is between 1.3 and 1.7%, which is less than in LDA as expected.

The O···H distances are between 1.3 and 2.0 Å, which is generally found in ab initio calculations [11] for hydrogen bonds. This is a first indication as far as the calculations are concerned that there are indeed hydrogen bonds which play an important role in the interchain bonding.

4.1. Electronic structure

As the Car–Parrinello technique uses the electronic structure to calculate forces, the electronic properties are easily accessible. The bandstructure for the monoclinic unit cell with the LDA functional to describe the exchange-correlation energy is presented in Fig. 4. Although the bandstructure was obtained by the Car–Parrinello method, the obtained results will be interpreted in the framework of

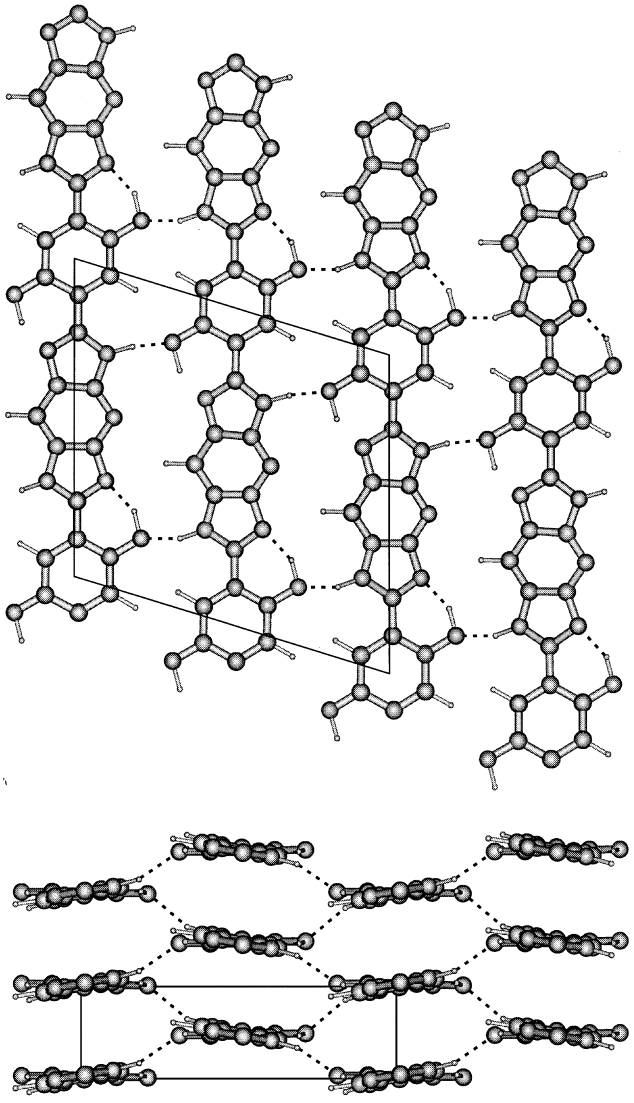

Fig. 3. The projection of the atomic positions in the monoclinic unit cell onto the *ac*-plane (top) and *ab*-plane (bottom).

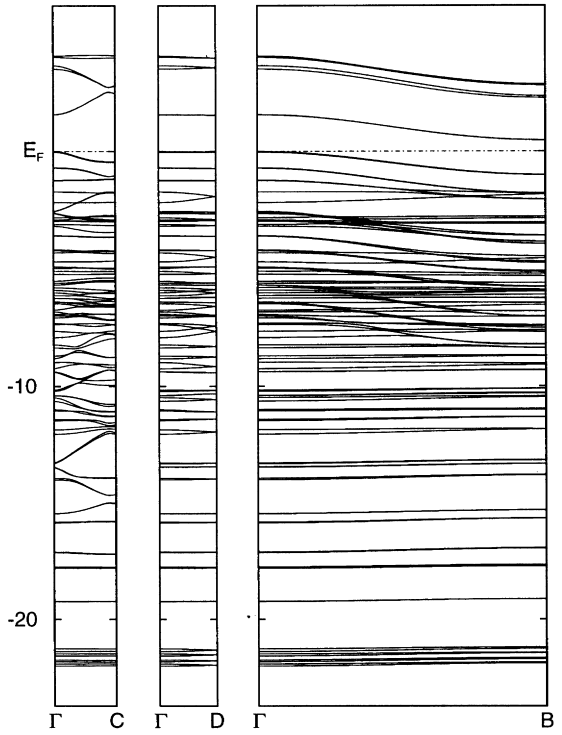

Fig. 4. The bandstructure of the monoclinic cell in three directions, all starting in Γ. C is the point at the Brillouin zone edge in the chain direction, B in the *b*-direction and D in the direction perpendicular to the chain, which corresponds to the diagonal direction.

Slater–Koster [21]. This powerful LCAO scheme directly relates dispersions of energy bands in a certain direction in the reciprocal space with the interatomic interactions in the corresponding direction in real space.

We can distinguish three important directions, one is the chain direction (Γ–C) and two are perpendicular to the chain (Γ–B and Γ–D). Γ–B is the direction along the *b*-axis, which is the direction of the $\pi-\pi$ interchain interaction. Γ–D is the direction along the diagonal of the unit cell, hence pointing from the centre of one chain towards the centre of the next-nearest chain, which is also approximately the direction of the hydrogen bonds.

That there are dispersions in the chain direction is no surprise as PIPD is a conjugated polymer. The comparable dispersion and hence the comparable interaction in the Γ–B direction, however, is somewhat surprising. The width of the top of the valence band in PIPD is 1.0 eV and therefore the interaction is 0.5 eV. This results from the $\pi-\pi$ interaction, as in graphite perpendicular to the graphite planes. For graphite [22], the $\pi-\pi$ interaction is 1.0 eV which is larger due to the shorter distance between the ring systems in graphite 3.34 Å, versus 3.48 Å in PIPD.

From the dispersion curve in the Γ–D direction (largest dispersion 0.56 eV), one can see that the interaction due to the hydrogen–oxygen interaction is smaller than the $\pi-\pi$ interaction.

4.2. Bonding

Although the previous paragraph suggests that the $\pi-\pi$ interaction is the dominating interchain interaction, it is important to realize that interaction is not the same as bonding. Bonding is the sum of all interactions, bonding as well as anti-bonding. Thus, while interactions can be strong, no net bonding necessarily results. Thus, while strong $\pi-\pi$ interactions exist, no strong net bonding occurs. This is also visible in Fig. 4. All bands which do show dispersion have the same derivative and thus no net bonding occurs in the first approximation.

In order to elucidate this point, we plot in Fig. 5 the calculated electron density in the *xz* plane for $y = 0$ and $y = 1/4$. Contours are plotted for the densities $\rho = 0.015\cdot(\sqrt[8]{10})^n$ for $n = 0$ to 9 in both cases. The $y = 0$ plane has the first chain in it and is positioned exactly between the chains at $y = 1/2$ and $y = -1/2$. The contours visible are clearly localised on the $y = 0$ chain (since the purpose of this picture is the visualisation of the interchain interactions we have suppressed contours of higher electron densities in order to enhance visibility). The $y = 1/4$ plot clearly shows the charge density of the hydrogen bonds. It should be stressed that the contours in both pictures are identical, and thus directly demonstrate the importance of the hydrogen bonds with respect to the $\pi-\pi$ overlap of the backbones.

To calculate the different energy contributions to the interchain bonding, different structures were compared. The total energy per chain in the monoclinic cell (E_X) can be written in the following way

$$E_X = E_{SC} + E_{\pi-\pi} + E_H + E_R \quad (2)$$

where E_{SC} is the energy of the isolated deformed chain, $E_{\pi\text{-}\pi}$ the energy which results from the stacking of the molecular chains in the *b*-direction, E_H the energy contribution of the hydrogen bonding network and E_R the energy resulting from other interchain interactions between the chains in the unit cell.

The contributions to formula (2) energies were determined by the following set of self-consistent calculations:

i. E_{SC}: This energy was calculated from a super cell with $b = 4.7$ for a single isolated chain with the geometry of the chain fixed as in the monoclinic crystalline case.
ii. $E_{\pi-\pi}$: The energy $E_{SC} + E_{\pi\text{-}\pi}$ was calculated from the same cell as (i) but with the length of the *b*-axis of the actual crystalline polymer. Only one chain per unit cell is present, stacked parallel along the *y*-direction. No external hydrogen bonds are possible here. The difference between the total energies calculated in (i) and (ii) leads to $E_{\pi\text{-}\pi}$.

In order to separate the individual contributions E_R and $E_{H,}$ we proceeded as follows: in the polymer PIPD the possibility of external hydrogen bonds was suppressed by replacing the NH groups by isoelectronic oxygen at the position of the nitrogen atom, fixing the geometry of the

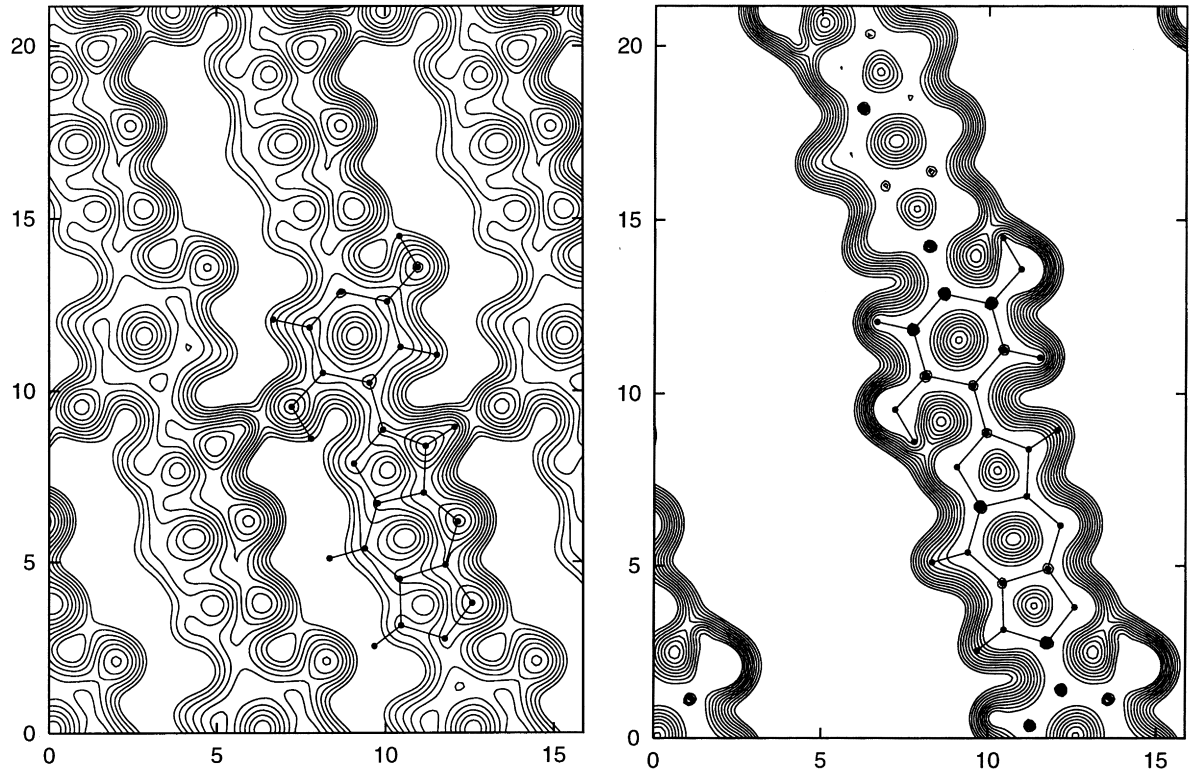

Fig. 5. The electron density in the *ac* planes for $b = 1/4$ (left) and $b = 0$ (right). The contour lines which are plotted are described by $\rho = 0.015\cdot(\sqrt[9]{10})^n$ for $n = 0$ to 9. The projection of one monomer on the *ac*-plane is drawn to clarify the picture. The axes are labelled in Å.

polymer. For this system, the crystal energy can be decomposed in

$$E^0_X = E^0_{SC} + E^0_{\pi-\pi} + E^0_R \quad (3)$$

as for PIPD. The set of calculations was repeated for this system.

iii. $E^0_{\pi-\pi}$: The energy was determined by the difference in the total energies of the isolated chain E^0_{SC} and the system of the unit cell with the actual value of the *b*-axis, containing one chain only. $E^0_{\pi-\pi}$ differs only 3% from the value obtained for $E_{\pi\text{-}\pi}$, justifying this united atom approach to determine interchain bonding.

iv. E^0_X: The energy was determined from the actual unit cell of PIPD with the NH groups replaced by oxygen, which allowed the determination of E^0_R. This value is assumed to be a good approximation of E_R.

The values obtained for the energies are listed in Table 3.

From this we find that the energy per chain of hydrogen bonding network is 0.98 eV, which is nearly 5 times the energy contribution of the π-π stacking. The hydrogen bonding network results in a bonding energy which is 1.7 times the bonding energy due to other interchain interactions. So the addition of the hydrogen bonding network results in a rigid-rod polymer with approximately three times stronger interchain bonding, which leads to better compressive properties.

The form of the hydrogen bonding network in the monoclinic cell can be seen in the projection of the optimised geometry on the *ac*-plane in Fig. 3. Hydrogen bonds can be found in both diagonal directions and a two-dimensional network is formed.

4.3. HOMO, LUMO, optical and electronic properties

From the bandstructure, it is clear that the bandgap in PIPD is indirect. The maximum of the valence band (HOMO) is situated at Γ. Its electron density is shown in Fig. 6. The bottom of the conduction (LUMO) band is located at B in the Brillouin zone. Fig. 7 shows its corresponding contour plot. The physical origin of the indirectness of the bandgap

Table 3
Results for the energy contributions as described in Eq. (2) and Eq. (3). The energy of the isolated deformed chain (E_{SC}) is taken as reference energy

	Energy per chain (eV)
E_X	−1.5694
E_{SC}	0.0000
$E_{\pi\text{-}\pi}$	−0.2013
$E_H + E_R$	−1.3681
E^0_X	−294.4291
E^0_{SC}	−293.8348
$E^0_{SC} + E^0_{\pi\text{-}\pi}$	−294.0418
$E^0_{\pi-\pi}$	−0.2070
E^0_R	−0.3873
E_H	−0.9808

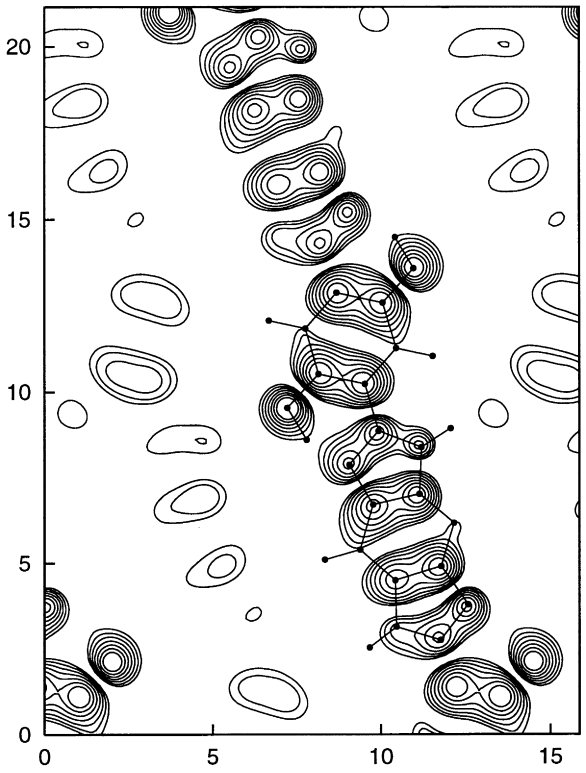

Fig. 6. The electron density plot in the plane $b = 1/8$ of the highest occupied molecular orbital at Γ. The plotted contours correspond to $\rho = 0.000318 \cdot (\sqrt[8]{10})^n$ for $n = 0$ to 6.

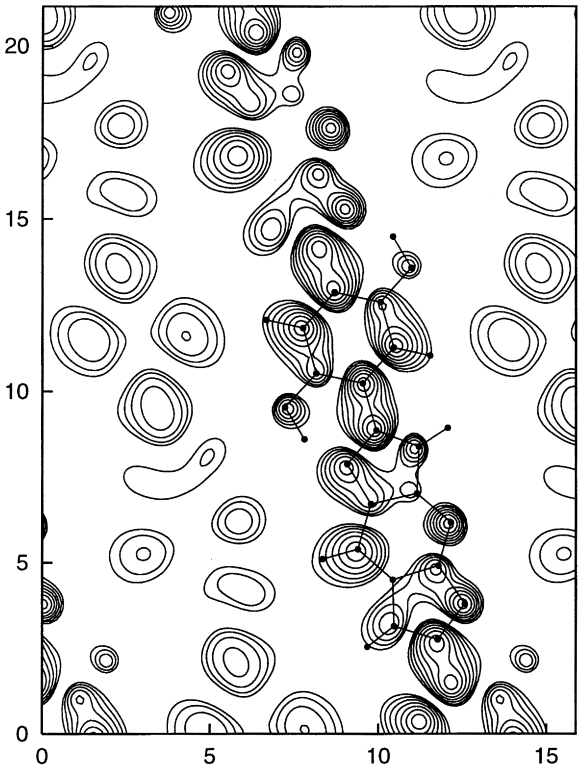

Fig. 7. The density plot in the plane $b = 1/8$ of the lowest unoccupied molecular orbital at B. The same contours are used as in Fig. 6.

is the strong $\pi-\pi$ interaction between the chains in the *y*-direction. Although, as has been explained before, this interaction does not result in a strong bonding, it has an influence on the bandstructure. The direct bandgap at Γ, which leads to direct transitions, is 1.57 eV. The indirect bandgap is 0.47 eV. It should be realized that LDA tends to underestimate bandgaps, so the actual bandgap may be larger by up to a factor of two. The bandgap for the isolated chain is direct, of course, and amounts to 1.26 eV.

The effective mass of holes upon doping with acceptors can be estimated from the curvature of the dispersion curve at the top of the valence band at Γ. It is directly clear from Fig. 6 that the effective mass depends greatly on the direction. The hole masses for the chain direction, the $\pi-\pi$ direction and the diagonal direction are respectively, 0.21, 1.2 and 7.1 m_e, where m_e is the free-electron mass.

The curvature at the bottom of the conduction band at *B* gives the electron mass in the chain direction of 0.14 m_e, in the $\pi-\pi$ direction of 1.3 m_e and in the diagonal direction of 16 m_e. Hence the electron mass changes two orders of magnitude with direction.

The electron mass for the isolated chain is in the chain direction 0.15 m_e and the hole mass is 0.35 m_e.

The masses in the chain direction are comparable with the masses found for poly-(phenylene vinylene) (PPV) which are of the order of 0.1 m_e [23]. There is, however, a clear difference between PPV and PIPD. In the isolated PPV chain, the lowest conduction band and the highest valence band are symmetric around the centre of the gap, which reflects in equal hole and electron masses. This electron-hole symmetry is partially removed in the crystal due to chain–chain interactions. In PIPD, the hole mass in the chain direction is for the single chain 2.3 times the electron mass, and in the crystal structure 1.5 times the electron mass. Hence there is no electron-hole symmetry for PIPD, neither in the single chain, nor in the crystal. For this reason, a PIPD conductor doped with donors would be more efficient than one doped with acceptors.

5. Triclinic PIPD

As mentioned before, there is another crystal structure which gives rise to the same XRD pattern. This is the triclinic structure with lattice constants $a = 6.68$ Å, $b = 3.48$ Å, $c = 12.02$ Å, $\alpha = 84°$, $\beta = 110°$ and $\gamma = 107°$. The unit cell contains only one monomer, and the *c*-axis is once again the chain axis. The triclinic unit cell is smaller than the monoclinic unit cell and hence the Brillouin zone is larger. Since the density of k-points determines the accuracy of the Brillouin Zone averages, more k-points are necessary to obtain good accuracy. A k-point set of 8 k-points was taken for this triclinic structure (referred to as Tric).

A third structure was used to calculate the energy difference. This structure was described in a non-primitive triclinic unit cell with the same dimensions as the

Table 4
Some important bond lengths and the torsion angle for the triclinic structures

Bond	Tric			Tric2			Comment
	LDA	GGAII	BP	LDA	GGAII	BP	
C–C	1.378–1.423	1.381–1.427	1.389–1.442	1.381–1.418	1.382–1.422	1.390–1.437	In DIP group
C–C	1.429	1.430	1.429	1.430	1.432	1.431	Between rings
O–H	1.067	1.045	1.056	1.059	1.039	1.051	N side
O–H	1.100	1.074	1.087	1.094	1.069	1.083	CH side
H···N	1.551	1.561	1.561	1.563	1.589	1.577	N side (intra)
H···N	1.447	1.472	1.468	1.459	1.490	1.483	CH side (intra)
N–H	1.051	1.037	1.053	1.044	1.030	1.047	N side
N–H	1.046	1.032	1.047	1.045	1.031	1.0457	CH side
H···O	1.853	1.851	1.814	1.836	1.849	1.796	CH side (inter)
H···O	1.829	1.829	1.777	1.902	1.913	1.862	N side (inter)
Torsion angle	8.3	8.2	8.1	7.1	7.1	7.2	

monoclinic unit cell. Since the unit cell parameters are identical to those of the monoclinic structure, the same k-point set can be used and the same systematic errors will occur in the total energy. Hence, these systematic errors will cancel in the energy difference. The corresponding primitive unit cell has lattice parameters $a = 6.48$ Å, $b = 3.48$ Å, $c = 12.01$ Å, $\alpha = 90°$, $\beta = 107°$ and $\gamma = 105°$. These show close resemblance to the Tric structure and can therefore be used in the energy comparison. We will refer to this structure as Tric2 and to the monoclinic structure as Mono.

Important bond lengths for both the Tric structure and the Tric2 structure are listed in Table 4 for all three functionals to describe the electron–electron interactions. Once again, there were no large changes in the distances and angles in the backbone and there was no difference between the distances in Tric2 and those in Mono. There was a difference in the torsion angle between the Mono structures (10°) and the Tric structures (7–8°), caused by an out-of-plane rotation of the Ph group over 2–3°.

The main difference between the Tric structures and the Mono structure is the form of the hydrogen bonding network. To visualise this, the projection of the Tric structure on the *ab*-plane is shown in Fig. 8 and one can clearly see that for this structure the hydrogen bonding network connects only chains which are in one diagonal plane. This could be regarded as a one-dimensional hydrogen bonding network, in contrast to the two-dimensional network of the monoclinic structure.

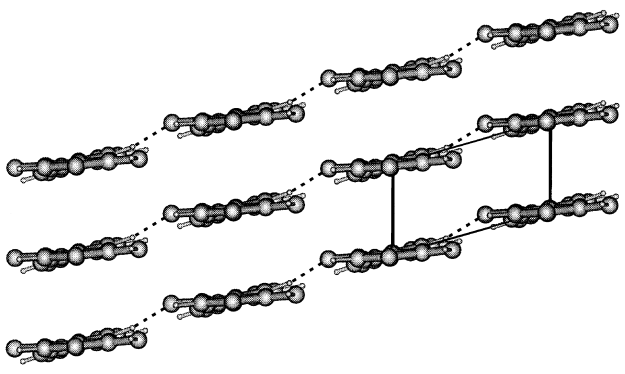

Fig. 8. The projection of the geometry in the triclinic structure on the *ab*-plane, which shows the one-dimensional character of the hydrogen bonding network.

As mentioned before, the Tric2 structure was chosen to allow a comparison between the energies of the Tric structures and the Mono structure. The energy differences between the structures was 76 meV, with Tric2 having the lower energy. This difference corresponds to an energy of 16 K/atom, which is very small especially if one realizes that the lattice parameters were not optimised.

These calculations do not allow any conclusions as to which crystal structure will be found in the actual fibres, and both structures might (co-)exist at room temperature.

6. Exchange correlation functionals

As we used different exchange-correlation functionals to study PIPD, it is appropriate to summarise the differences between them. There is a clear difference between LDA and the two gradient corrections, in that the overestimation of the bond strengths in LDA is removed by the GCs, which results in longer bond lengths for the GCs. The difference between the two GCs is not large, but in general BP leads to the weakest bonds. The same is true for the hydrogen bonds. The weakening is also found in the elastic modulus, which is clearly lower for the GCs.

The most dramatic effect was found by comparing the monoclinic crystal with the single chain. The energy differences per atom for LDA, GGAII and BP were, respectively, 592, 111 and 37 K/atom. If these energies are interpreted as a scale of temperature and compared with the temperatures at which X-ray experiments [2] could be performed (as high as 700 K), then LDA seems to be the most reliable. The reduction of the intermolecular

bonding for the GCs is in agreement with the results for benzene [24] and for polyethylene [25]. The reduction of the interchain interaction can also be found in the reduction of the indirect bandgap, 0.47 eV in LDA compared to 0.52 eV for GGAII. The direct bandgap, however, is not affected.

To summarise, LDA produces reasonable results for intrachain and interchain properties, but suffers from overbounding. Gradient corrections reduce the strength of the bonds but overcompensate in the case of intermolecular properties.

7. Conclusions

In this article, we have presented the first ab initio calculations on the novel rigid-rod polymer PIPD using density functional techniques. The behaviour of the molecular chain under strain is studied and the chain modulus agrees excellently with experiment.

Two crystal structures are studied and hydrogen bonding networks proposed earlier from XRD results [2] are demonstrated to exist: a sheet-like network for the triclinic structure and a two-dimensional network for the monoclinic structure. Negligible energy differences were found and both structures are expected to exist at room temperature.

The Car–Parrinello technique provides accurate forces and related properties, and also electronic properties. The optical and electronic structure are discussed. These revealed a large $\pi-\pi$ interaction, but with a weak bonding. The hydrogen bonds show less interaction, but result in a nearly five times stronger bonding. The improvement in the compressive strength of PIPD compared to PBO and PBT can indeed be attributed to the hydrogen bonding network, as the interchain bonding of PIPD is approximately three times the bonding without the network.

Acknowledgements

The authors wish to thank Dr. E.A. Klop of Akzo Nobel Central Research for providing the XRD results and for fruitful discussions, and Dr. D.J. Sikkema and Dr. M.G. Northolt for their interest in the results of this work. This work is part of the research program of the Stichting Fundamenteel Onderzoek der Materie (FOM) with financial support from the Nederlandse Organisatie voor Wetenschappelijk Onderzoek (NWO) and has benefited from the Ψ_k-network.

References

[1] Sikkema DJ, to appear in Polymer.
[2] Klop EA, Lammers M, to appear in Polymer.
[3] Lammers M, Klop EA, Northolt MG, Sikkema DJ, to appear in Polymer.
[4] Hageman JCL, Meier RJ, Heinemann M, de Groot RA. Macromolecules 1997;30:5953; Hageman JCL, de Groot RA, Meier RJ. Computational Materials Science 1998;10:180.
[5] Hageman JCL, de Groot RA, in preparation.
[6] Welsh WJ, Bhaumik D, Mark JE. Macromolecules 1981;14:947.
[7] Ambrosch-Draxl C, Majewski JA, Vogl P, Leising G. Phys Rev B 1995;51:9668.
[8] Ceperley DM, Alder BJ. Phys Rev Lett 1980;45:566.
[9] Perdew JP, Chevary JA, Vosko SH, Jackson KA, Pederson MR, Singh DJ, Fiolhais C. Phys Rev B 1992;46:6671.
[10] Becke AD. Phys Rev A, 1988;38:3098; Perdew JP. Phys Rev B, 1986;33:8822.
[11] Sim F, St-Amant A, Papai I, Salahub DR. J Am Chem Soc 1992;114:4391.
[12] Dal Corso A, Pasquarello A, Car R, Baldereschi A. Phys Rev B 1996;53:1180.
[13] Bockstedte M, Kley A, Neugebauer J, Scheffler M. Comp Phys Comm 1997;107:187; Fuchs M, Scheffler M. Comput Phys Commun, to be published; Gonze X, Käckell P, Scheffler M. Phys Rev B, 1990;41:1264.
[14] Kohn W, Sham LJ. Phys Rev 1965;140:A1133.
[15] Payne MC, Joannopoulos JD, Allan DC, Teter MP, Vanderbilt DH. Phys Rev Lett 1986;56:2656.
[16] Troullier N, Martins JL. Phys Rev B, 1991;43:1993.
[17] Kleinman L, Bylander DM. Phys Rev Lett, 1982;48:1425.
[18] Weast RC. Handbook of chemistry and physics. Baton Rouge, FL: CRC Press, 1981, 62nd ed.
[19] van der Horst JW. MSc. thesis, Nijmegen University, The Netherlands, 1997.
[20] The final experimental lattice parameters [2] differ slightly from the values presented here, but the effect of this difference will be small.
[21] Slater JC, Koster GF. Phys Rev 1954;94:1498.
[22] Charlier JC, Gonze X, Michenaud JP. Phys Rev B 1991;43:4579.
[23] Gomes da Costa P, Dandrea RG, Conwell EM. Phys Rev B 1993;47:1800.
[24] Meijer EJ, Sprik MJ. Chem Phys 1996;105:8684.
[25] Montanari B, Jones RO. Chem Phys Lett 1997;272:347.